ORIGINAL ARTICLE

Enhanced complement activation and MAC formation accelerates severe COVID-19

Calder R. Ellsworth[1,2] · Zheng Chen[1,2] · Mark T. Xiao[1,2] · Chaosi Qian[3] · Chenxiao Wang[1,2] · Mst Shamima Khatun[4] · Shumei Liu[1,2] · Mohammad Islamuddin[1,2] · Nicholas J. Maness[1,2] · Jose A. Halperin[5] · Robert V. Blair[1] · Jay K. Kolls[4] · Stephen Tomlinson[3] · Xuebin Qin[1,2,6]

Abstract

Emerging evidence indicates that activation of complement system leading to the formation of the membrane attack complex (MAC) plays a detrimental role in COVID-19. However, their pathogenic roles have never been experimentally investigated before. We used three knock out mice strains (1. $C3^{-/-}$; 2. $C7^{-/-}$; and 3. $Cd59ab^{-/-}$) to evaluate the role of complement in severe COVID-19 pathogenesis. $C3$ deficient mice lack a key common component of all three complement activation pathways and are unable to generate C3 and C5 convertases. $C7$ deficient mice lack a complement protein needed for MAC formation. $Cd59ab$ deficient mice lack an important inhibitor of MAC formation. We also used anti-C5 antibody to block and evaluate the therapeutic potential of inhibiting MAC formation. We demonstrate that inhibition of complement activation (in $C3^{-/-}$) and MAC formation (in $C3^{-/-}$. $C7^{-/-}$, and anti-C5 antibody) attenuates severe COVID-19; whereas enhancement of MAC formation ($Cd59ab^{-/-}$) accelerates severe COVID-19. The degree of MAC but not C3 deposits in the lungs of $C3^{-/-}$, $C7^{-/-}$ mice, and $Cd59ab^{-/-}$ mice as compared to their control mice is associated with the attenuation or acceleration of SARS-CoV-2-induced disease. Further, the lack of terminal complement activation for the formation of MAC in $C7$ deficient mice protects endothelial dysfunction, which is associated with the attenuation of diseases and pathologic changes. Our results demonstrated the causative effect of MAC in severe COVID-19 and indicate a potential avenue for modulating the complement system and MAC formation in the treatment of severe COVID-19.

Keywords Complement · C3 · MAC · Cd59 · Severe COVID-19 · Endothelial dysfunction

✉ Xuebin Qin
  xqin2@tulane.edu

1 Tulane National Primate Research Center, Covington, LA 70433, USA

2 Department of Microbiology and Immunology, Tulane University School of Medicine, New Orleans, LA 70112, USA

3 Department of Microbiology and Immunology, Medical University of South Carolina, and Ralph Johnson VA Medical Center, Charleston, SC, USA

4 Departments of Medicine and Pediatrics, Center for Translational Research in Infection and Inflammation, Tulane University School of Medicine, New Orleans, LA 70112, USA

5 Division of Hematology, Department of Medicine, Brigham and Women's Hospital, Boston, MA, USA

6 Division of Comparative Pathology, Tulane National Primate Research Center, Health Sciences Campus, 18703, Three Rivers Road, Covington, LA 70433, USA

Introduction

SARS-CoV-2 infection mediates massive activation of the host immune system and drives uncontrolled inflammation that affects multiple organs, causing severe COVID-19 [1, 2]. The complement system, a key component of innate immunity, provides a first line of defense against infection; however, it has been implicated in playing a detrimental role in COVID-19 pathogenesis by accelerating lung and other tissue damage [1]. These underlying mechanisms remain unclear and require further experimental investigation [1, 3, 4].

The complement system comprises of 50 + soluble and membrane-bound proteins and is activated primarily via one of three distinct pathways (classical, lectin and alternative pathways) [1, 5, 6]. All three pathways converge at C3 cleavage, with the generation of C3b and C3a, and the subsequent formation of C5 convertase. The C5 convertase then cleaves

C5 to form C5b and C5a [1, 5]. The soluble anaphylatoxins C3a and C5a have inflammatory and immune modulatory functions. The terminal complement activation pathway is initiated by C5b and ultimately results in the formation of the membrane attack complex (MAC) [6–9]. The MAC is a macromolecular pore capable of inserting itself into cell membranes and lysing foreign pathogens, heterologous cells and, under certain pathological conditions, autologous cells [1, 6, 7, 10, 11]. Additionally, the formation of MAC at sublytic concentrations in a cell membrane stimulates signaling cascades [12–20] that lead to the activation of monocytes and mediate inflammation [9, 21, 22]. To protect autologous cells from MAC attack, more than 10 plasma- and membrane-bound inhibitory proteins have evolved that restrict complement activation at different stages of each of the three pathways [5, 6]. CD59, the most important membrane-bound complement regulator, specifically inhibits MAC formation by preventing C9 incorporation and polymerization [23]. Extensive clinical evidence suggests that increased complement activation in the circulation and in the lungs during SARS-CoV-2 infection accelerates severe COVID-19 [1, 24–33]. Hospitalized COVID-19 patients have significantly higher levels of circulating sC5b-9 (soluble MAC or sMAC) as compared to influenza patients [31]. sMAC, C3a and C5a serum levels are associated with increased COVID-19 severity [34–39]. Heightened complement deposition has been found in various tissues of severe COVID-19 patients, including C3 and C5b-9 on lung endothelium and C5a in bronchoalveolar lavage fluid (BALF) [37, 40]. Recent studies have documented that enhanced complement activation, as indicated by increased MAC and C4d serum levels, during hospitalization is associated with a higher risk of 60-day mortality in SARS-CoV-2-infected patients[24]. Heightened complement activity also increases platelet activation contributing to thromboinflammation in severe COVID-19 patients [27, 41]. Additionally, various other non-respiratory viruses activate complement resulting in increased tissue damage, including ross river virus (RRV) and human immunodeficiency virus (HIV). In RRV infection, complement activation worsens inflammatory arthritis and myositis, as demonstrated using C3- and CR3-deficient mice [42]. In HIV infection, the virus both evades and activates complement to enhance infectivity. Deposition of C3 fragment onto HIV-1 virions and generation of C5a during the HIV infection facilitate HIV-1 interaction with cells such as monocytes/macrophages and dendritic cells [43–46]. To evade host detection and protect itself from complement-mediated virolysis, HIV uses glycoproteins to capture factor H and additionally incorporates the regulators CD55 and CD59 into the envelope after budding [47, 48]. Increased complement activation and complement product deposition in tissues such as the brain has been implicated in contributing to the pathogenesis of HIV-associated comorbidities such

as neurocognitive disorders [44]. Altogether, there is extensive evidence indicating that complement activation plays a detrimental role in COVID-19, RRV and HIV infection [1, 42, 44]. However, how complement activation contributes to the pathogenesis and whether the formation of the MAC accelerates severe COVID-19 remains unclear. Clinical trials with complement inhibitors indicate that modulation of complement activation may have a beneficial effect for treating severe COVID-19 [49–52]. The causative roles of complement activation and specifically the MAC in severe COVID-19 have not been experimentally investigated. This knowledge gap limits our ability to effectively modulate the complement system for the treatment of severe disease. To fill this gap, we used a murine COVID-19 model together with mice deficient in: (1) C3, the central component of all 3 activation pathways and upstream of MAC formation; (2) C7, a key complement component for MAC formation, but downstream of C3 activation and C3a and C5a generation; and (3) CD59, a membrane-bound MAC specific inhibitor. We also used a clinically relevant paradigm of C5 blockade using an anti-C5 mAb that blocks the generation of C5a and the MAC. To better understand pathological mechanisms, we performed scRNA-seq (single cell RNA sequencing) analysis in mouse model of COVID-19. We found that the inhibition of complement activation in $C3^{-/-}$ mice and suppression of MAC formation in $C3^{-/-}$ and $C7^{-/-}$ mice as well as with anti-C5 antibody treatment attenuates severe COVID-19 while enhancement of MAC formation in $Cd59ab^{-/-}$ mice, increases the severity of the disease.

Methods

Ethical compliance and animal models

Our research follows Tulane University's Institutional Animal Care and Use Committee-approved protocols (1557 and 1331) and complied with all relevant ethical regulations for animal treatment. Murine models were bred and housed within the university's animal facility. The following lines were sourced from the Jackon Laboratory (K18-hACE2$^{+/-}$ (034860), C57BL/6 J (000664), $C3^{-/-}$ (9,003,641), $C7^{-/-}$ (042133). $Cd59ab^{-/-}$ were generated by us previously [53–56].

SARS-CoV-2 virus and infection

The SARS-CoV-2 USA-WA1/2020 isolate (NR-52281) was sourced from the CDC through BEI Resources, NIAID, NIH and the CoV-2 MA30 Variant was acquired directly from Dr. Perlman [57]. Expansion of virus and inoculation of mice was performed at Tulane using the same methodology as described previously [58]. Mice were infected in Tulane

BSL3 core facility via intranasal inoculation and monitored in the morning for body weight and behavior daily. Mice were euthanized if they reached 25% body weight loss. Percent body weight (%BW) was calculated by measuring body weight at 0 DPI (BW_{0DPI}) and on subsequent days (BW_{XDPI}) using the following calculation: $\%BW = 100 - 100 \times (BW_{0DPI} - BW_{XDPI})/BW_{0DPI}$.

Hemolytic assay

We sourced whole blood from our mice via cardiac puncture and collected the serum by incubation at room temperature for 30 min in a BD microtainer before centrifugation and storage at –80 °C. The hemolytic assay was performed using Ab-sensitized sheep erythrocytes (Cat# B250, Complement Technology, Inc) and following the manufacturer's protocol using serial dilution of sample serum (2%, 4%, and 8%).

ELISA measurements

Following the protocols of the respective manufacturer, analytes from collected serum were measured in duplicate using the following ELISA kits and dilutions. C5a ELISA 1:50 dilution (R&D systems, DY2150), C3a ELISA 1:10 dilution (R&D systems, NBP2-70,037), VEGF ELISA 1:20 (R&D systems, MMV00-1), and vWF ELISA 1:5 dilution (LSBio, LS-F22891).

Administration of BB5.1 or IgG$_1$

Mice were treated via intraperitoneal treatment with 200 μL/mouse (40 mg/kg) of either Anti-C5 mAb BB5.1 (provided by Dr Steve Tomlinson) or IgG$_1$ isotype control (Leinco Technologies, Inc., I-536). Mice were treated on -1 DPI (24 h before infection), 0 DPI (2 h before infection), and 2 DPI.

Histopathological examination

Tissues were collected in formalin fixative and processed routinely for paraffin embedding. For histological studies, 5 μm lung tissue sections were either stained routinely with hematoxylin and eosin (H&E) or left unstained for immuno-histochemistry (fluorescent (FIHC) and chromogenic (IHC)). Once stained, slides were digitally imaged with Nanozoomer S360 scanner (H&E and IHC) or Axio Scan.Z1 (FIHC).

Quantification of pulmonary edema and inflammatory cell infiltration was performed by a board-certified veterinary pathologist using pattern recognition software (HALO AI 3.4, Indica Labs). A DenseNet.V2 neural network was used to train a tissue segmentation algorithm to detect pulmonary edema and cellular infiltration. Regions of interest were manually drawn around each lung section on a slide, and the algorithm was used to quantify edema and cellular infiltration within regions of interest. Results of the algorithm were checked for accuracy by the pathologist that trained the algorithm.

Bronchial epithelial damage was scored manually by a pathologist using a semiquantitative method assigning slides a score from absent (0) to severe (4 +). Scoring criteria were determined as follows: 0: no histopathologic evidence of bronchial epithelial damage; 1 + : < 10% of airways exhibited degenerative changes; 2 + : 10–25% of areas exhibited degenerative changes; 3 + : > 25% of airways exhibited degenerative changes; 4 + : > 25% of airways exhibited degenerative changes with segmental sloughing of airway epithelial cells. Degenerative changes include vacuolation, attenuation, apical blebbing, and sloughing.

Detection of viral RNA

SARS-CoV-2 N viral RNA from lung tissue samples were measured and quantified using qRT-PCR as described previously [58].

Immunohistochemical staining

Lung tissue sections were fixed in zinc formalin, embedded in paraffin, and then subjected to epitope retrieval using solutions of varying pH (Vector Labs H-3301 and H-3300) [33, 59]. Blocking was performed using BSA, goat serum, or donkey serum, followed by incubation with primary and secondary antibodies. Guinea pig anti-SARS S protein (NR-10361, BEI Resources) was used at a 1:1000 dilution. For Figs. 6 and supplemental 7 and the detection of deposits of MAC, polyclonal rabbit anti-rat C9 (obtained from Dr. Paul Morgan) was used at a 1:400 dilution as described in [55, 56, 60]. In Fig. 7, an antibody against C9 (USBiological Life Sciences, 362,359, Rabbit Anti-C9) was used at a 1:1000 dilution. C3 staining was performed using an anti-C3 antibody (catalog number 200999, Abcam) at a 1:1000 dilution. For C9 quantification, we used HALOv3.4 (Indica Labs). For C3 quantification, we used NIH Image J software and applied "Color deconvolution" by set vectors to "H DAB" to get the DAB-stained area and using the IHC Profiler plugin to automatically score the staining status of samples to obtain the percentage contribution of positive.

Single cell analysis

We mined gene differences in infected vs naïve B6 mice as described in attached supplementary material.

Statistics

Data representation was in the form of mean ± SEM. For multiple group comparisons over time, a two-way ANOVA with Tukey's post hoc test or mixed-effects analyses with Sidak's post hoc test were applied. For two-group comparisons, we used the unpaired Student's *t*-test, considering $p < 0.05$ as statistically significant. Survival analyses were performed using log-rank (mantel-cox) test.

Results

SARS-CoV-2 infection mediates increased systemic complement activation in mice

We first investigated whether SARS-CoV-2 infection mediates complement activation in C57BL/6 J (B6) mice infected with MA30, a mouse adapted strain established by Dr. Perlman [57]. In our previous studies [58], we established the lethal dose (LD: 2×10^5 TCID$_{50}$, a dose causing nearly 100% mortality), the LD$_{50}$ dose (5×10^4 TCID$_{50}$, a dose causing 50% mortality) and the sublethal dose (1×10^4 TCID$_{50}$, a maximal non-lethal dose) of MA30 in 12–20-week-old B6 mice. MA30 in B6 mice resulted in pulmonary pathology characterized acutely by bronchial epithelial degeneration and necrosis, pulmonary edema, and interstitial pneumonia [58]. To measure the dynamic changes of complement activity, we collected sera from B6 mice at 1 to 7 days post infection (DPI) with a sublethal dose. This dose resulted in a maximum 20% loss of body weight at 4 DPI together with major histological changes in the lungs of infected B6 as previously described [58]. To measure systemic complement activity in mouse serum by MA30 infection, we used a well-described hemolytic assay to measure MAC-mediated lysis of antibody-sensitized sheep erythrocytes [61]. After infection, there was progressively reduced complement activity in mouse serum collected at 0, 2, 4 and 7 DPI, indicating ongoing systemic complement activation during SARS-CoV-2 infection (Fig. 1A). Furthermore, we found that infected male and female B6 mice had significantly higher levels of C3a and C5a in serum compared with naïve B6 counterparts (Figs. 1B and C). Infected males had higher C3a but not C5a levels in serum compared to infected females (Figure S1A-B). This result further confirms that SARS-CoV-2 infection mediates complement activation and reduces serum complement levels.

Our previous global transcriptomic analyses of a SARS-CoV-2-infected human ACE2 (hACE2)-transduced mouse model and hACE2-transgenic mouse models documented that SARS-CoV-2 infection mediates the up-regulation of complement components and the activation of complement in the infected lung [32, 33, 59, 62]. To further dissect the up-regulation of complement components during infection, we mined our previous single-cell RNA sequencing data from the MA30-infected B6 mice at 2 DPI [63]. We found that *C1qa, C1qb, C1qc, C4a, C4b, C2, C3* and *Cfb,* but not *C7* and *C9*, were significantly upregulated in either the macrophages, neutrophils, and endothelial cells of MA30-infected lungs as compared to naïve mice (Fig. 1D–G and Figure S2). Thus, up-regulated complement genes in the infected lung are associated with ongoing complement activation.

Deficiency of C3 protects against severe COVID-19

To explore the role of complement activation in severe COVID-19, we infected C3 deficient ($C3^{-/-}$, $n = 9$) and sufficient ($C3^{+/+}$ or B6, $n = 9$) mixed-sex mice at 14-weeks old with an LD$_{75}$ of MA30 strain (5×10^4 TCID$_{50}$) and monitored them from 0 to 12 DPI. We euthanized some of the mice for analyzing lung pathological changes and viral load at 4–5 DPI (Fig. 2A–H). Infected $C3^{-/-}$ mice lost significantly less body weight from 0 to 5 DPI and had a significantly higher survival rate (100%) than infected $C3^{+/+}$ mice (Fig. 2A and B). We did not detect any significant differences in viral load and in viral S protein staining cells between the two groups (Fig. 2C and Figure S3A-B). Absence of complement activation in infected $C3^{-/-}$ mice in a separate all-male cohort was confirmed by lower serum C3a and C5a levels in infected $C3^{-/-}$ compared to $C3^{+/+}$ males at 3 DPI (Fig. 2D and E), and further confirmed by low or absent serum hemolytic activity (Fig. 2F). Histologically, we found that the infected $C3^{-/-}$ mice, from the original mixed-sex group, showed significantly reduced pulmonary edema as compared with the infected $C3^{+/+}$ mice (Fig. 2G-H). We have previously shown that rapid development of severe pulmonary edema is associated with outcome in MA30-infected C57BL/6 mice (B6) [58]. Bronchial epithelial degeneration also tended to be lower in $C3^{-/-}$ mice ($P = 0.08$). Taken together, these results indicate that deficiency of C3 protects against severe COVID-19 in MA30-infected B6 mice.

To confirm these results we used another severe COVID-19 model, namely the hACE2-transgenic K18 mouse model ($K18$-$hACE2^{+/-}$) [32, 62]. We crossed $C3^{-/-}$ mice with $K18$-$hACE2$ mice ($C3^{-/-}/K18$-$hACE2^{+/-}$) and infected them with SARS-CoV2-WA1 (the USA-WA1/2020, a strain ancestral to the Wuhan variant) [32, 62]. C3 deficiency in hACE2-$K18^{+/-}$ mice protected against the development of severe COVID-19 regardless of the viral load, as evidenced by less body weight loss and lung edema levels despite similar viral subgenomic N RNA in the infected $C3^{-/-}/K18$-$hACE2^{+/-}$ mice as compared to $C3^{+/+}/K18$-$hACE2^{+/-}$ mice (Fig. 3A-C). These results further demonstrate that deficiency of C3 protects against severe COVID-19 in mice.
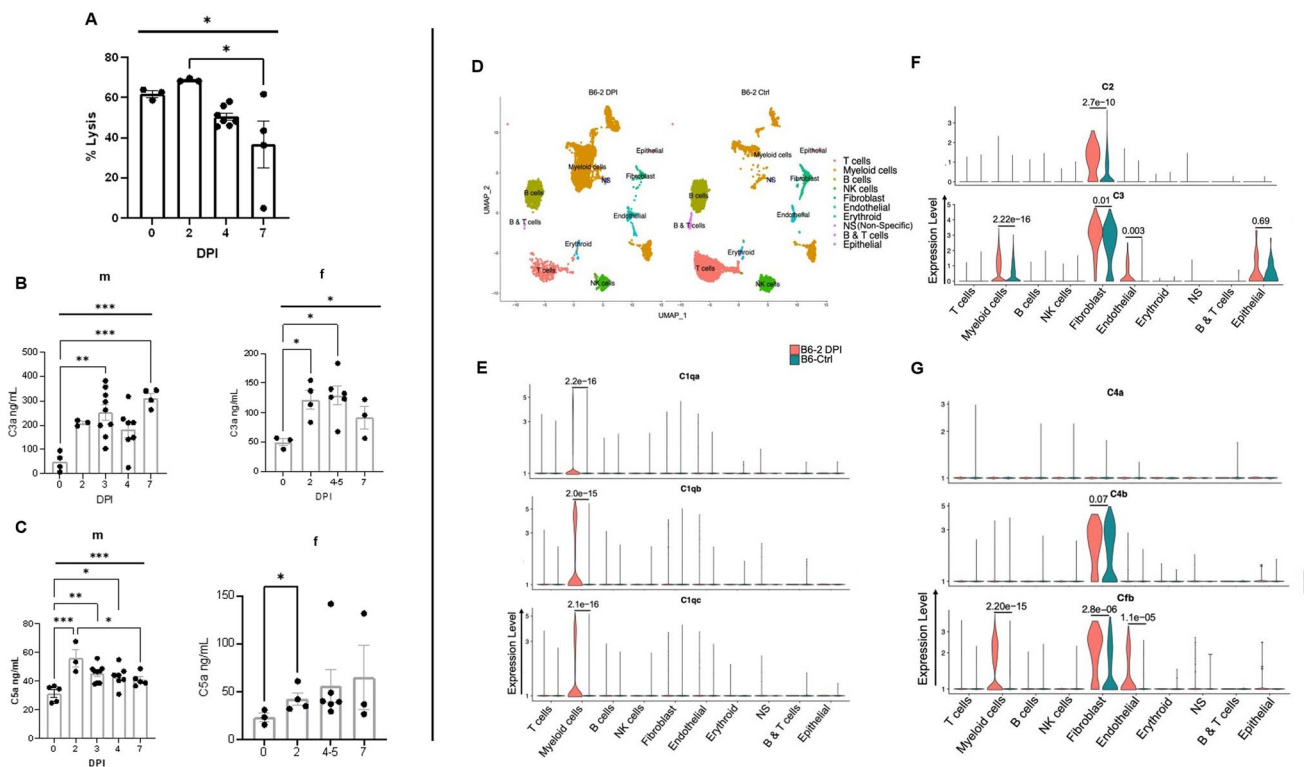
Fig. 1 SARS CoV2 infection mediates increased systemic complement activation and up-regulates complement transcripts in multiple pulmonary cells in mice. **A** Complement-mediated hemolytic activity in the infected MA30-infected mice. The 4% of serum was collected from 14-16 weeks old males at different days post infection (DPI) with sublethal dose of SARS-CoV-2 MA30 (2.5×10^4 TCID$_{50}$), and were used as source of complement to measure MAC-mediated hemolysis of the antibody-sensitized sheep erythrocytes. **B–C** C3a level (**B**) and C5a (**C**) detected by sandwich ELISA from sera of male (m) and female (f) mice collected after infection with sublethal (2.5×10^4 TCID50) and lethal (5×10^4 TCID$_{50}$) doses of SARS-CoV-2 MA30. Overall significances shown in Figure 1A-1C were analyzed by one-way ANOVA and were indicated with horizontal bar, with group comparisons by Tukey test, * $p < 0.05$, ** $p < 0.01$, and ***$p < 0.001$, and **** $p < 0.0001$. **D** Major clusters and respective cell types for two 12-week-old female MA30 infected *B6* mice (1×10^4 TCID$_{50}$) at 2dpi and two 12-week-old non-infected *B6* mice by scRNA-seq data. Uniform manifold approximation and projection (UMAP) for dimension reduction plot with major cell types of scRNA-seq. Single-cell suspensions from whole infected lungs at 2 dpi and non-infected lungs were processed and sequenced. We identified 10 major clusters including T cells, myeloid cells, B cells, NK cells, fibroblast, endothelial, erythroid, non-specific, B & T cells, epithelial cells. **E–G** Expression of *C1qa, C1qb, C1qc, C2, C4a, C4b,* and *Cfb* in the infected (pink) and non-infected (teal) cell clusters of lungs with *p*-values indicated

The deficiency of CD59 exacerbates COVID-19, whereas the inhibition of the MAC mitigates severe manifestations of the disease

To explore the pathogenic role of the MAC in severe COVID-19, we used mice sufficient and deficient in CD59, a key MAC-specific regulator [55, 56]. In mice, there are two CD59 GPI-linked proteins (*CD59a* [64] and *CD59b* [65]) while humans express only one CD59. *Cd59a* is the primary source of CD59 anti-MAC activity in mice under physiological conditions [66, 67]. *Cd59b* is expressed at a lower level on erythrocytes and at a higher level on testis compared to *Cd59a* [68–70]. To eliminate any potential compensatory effects of *Cd59a* and *Cd59b*, we used our previously generated and characterized *Cd59ab* double knockout (*Cd59ab*$^{-/-}$) [53, 54] mice, which we infected with a non-lethal dose of MA30 (1×10^4, IN), in parallel with CD59 sufficient (*Cd59ab*$^{+/+}$) mice. Infected male and female *Cd59ab*$^{-/-}$ mice lost a greater percent of body weight and had a higher mortality rate compared to infected *Cd59ab*$^{+/+}$ counterparts, while both types of mice had similar lung viral load and S protein staining (Fig. 4A-C and S4). Histologically, we found that *Cd59ab*$^{-/-}$ mice exhibited more severe pulmonary edema than *Cd59ab*$^{+/+}$ mice (Fig. 4D-E). Bronchial epithelial degeneration was also significantly increased *Cd59ab*$^{-/-}$ mice (Figure S5A-C); whereas interstitial inflammatory cell infiltrate was similar between CD59 sufficient and deficient mice.

To test the potential therapeutic effect of inhibiting MAC formation in severe COVID-19 we used BB5.1, an anti-mouse C5 antibody and functional homologue of the clinically used drug eculizumab [55]. Eculizumab is used for treating paroxysmal nocturnal hemoglobinuria (PNH) by blocking MAC formation and C5a production and has
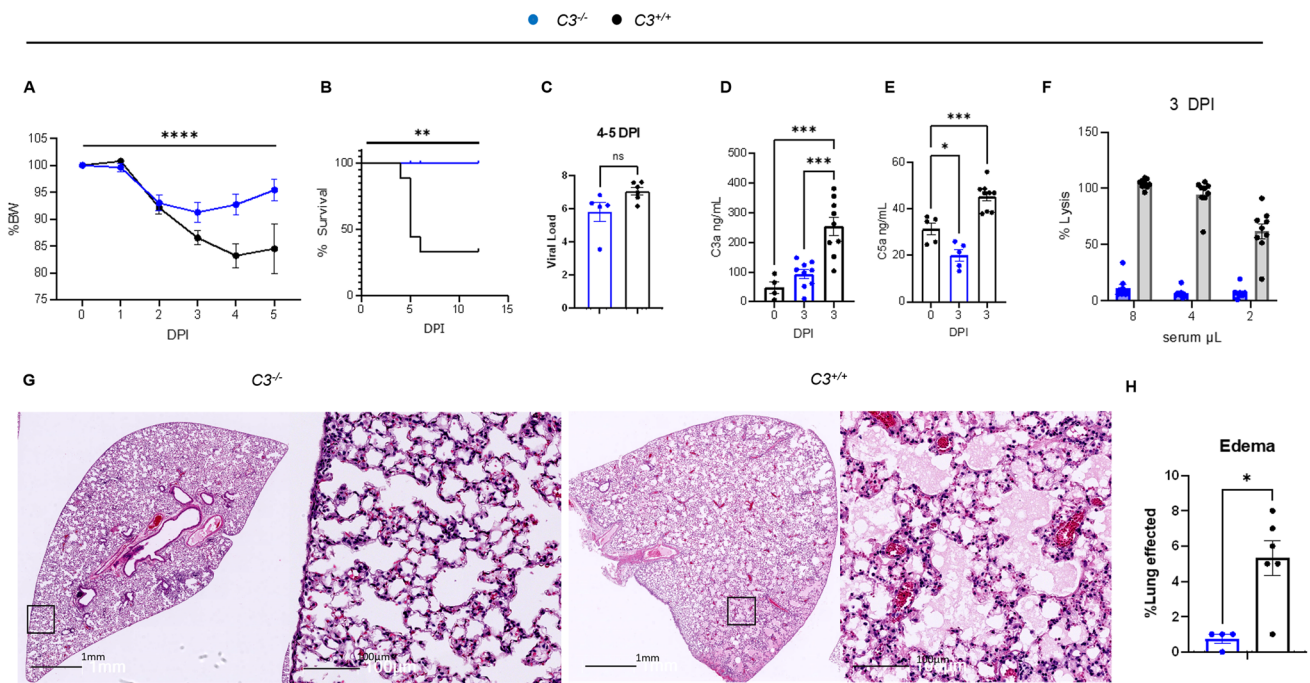
Fig. 2 Deficiency of C3 protects against severe COVID-19 in MA30-infected B6 mice. **A–C** and **G–H**: $C3^{-/-}$ and $C3^{+/+}$ mice (n=9/group) aged 14 weeks and of mixed sex (5 males and 4 females per goup) were infected with a lethal dose of MA30 (5×10^4 $TCID_{50}$) and sacrificed at 4–5 and 12 DPI. Percent body weight (**A**) and survival rate (**B**) after the infection were analyzed by Two-way ANOVA and survival by Log rank (Mantel-Cox) test. **C** Viral load was quantified by measuring subgenomic N RNA by qPCR in the mice at 4-5 DPI. **D–F** 9 $C3^{-/-}$ and 9 $C3^{+/+}$ male mice were infected with MA30 5×10^4 $TCID_{50}$ and were sacrificed at 3DPI for tissue collection. C3a (**D**) and C5a (**E**) serum levels as quantified by sandwich ELISA. Statis-tics show significance between groups using One-way ANOVA with Tukey's multiple comparisons. Of note, there is a non-specific C3a signal in $C3^{-/-}$ mice, which may be the result of sample hemolysis and non-specific binding. **F** Complement activity measured by hemolytic assay with exposure of serial dilution of sera from C3 sufficient and deficient mice at 3 DPI to antibody sensitized sheep erythrocytes. **G–H** Representative images (**G**) of edema from C3 sufficient and C3 deficient mice after infection at 4-5DPI, and quantification (**H**) by two-tailed student T-test. * $p < 0.05$, ** $p < 0.01$, ***$p < 0.001$, and **** $p < 0.0001$ by the respective statistical methods as detailed above

resulted in significant improvements in survival and a reduction in complications for PNH patients [71]. Previously, we [55] and others [15] have documented that the inhibition of MAC formation with the treatment of BB5.1 protects against the development of atherosclerosis without any evident adverse effect on the mice. Specifically, in this study, we administered $Cd59ab^{-/-}$ mice (in B6 background) with anti-C5 mAb clone BB5.1 or IgG isotype control clone 135.8 (40 mg/kg/day, i.p.) on days 0–2, followed by twice a week on days 3–60 for atherosclerosis study [55]. Here, we used the same dose regimen by treating $Cd59ab^{-/-}$ mice with BB5.1 or IgG isotype control for two consecutive days (40 mg/kg/per day, IP), followed by inoculation with a non-lethal dose of MA30. At 2 DPI, the infected mice were treated again with BB5.1 or IgG isotype. Despite a similar viral load, the BB5.1 treated mice lost significantly less body weight and had similar survival rates as compared to IgG-treated mice (Fig. 4F-G). As expected, serum collected from infected BB5.1-treated mice had a lower complement-mediated hemolytic capacity and lower C5a levels as compared with serum collected from infected IgG-treated mice

(Fig. 4H-I). Thus, inhibition of MAC formation by BB5.1 treatment partially protected against the development of severe COVID-19 in this model but could not significantly prevent fatal outcomes.

Deficiency of C7 protects against severe COVID-19

To conclusively establish the role of MAC in the pathogenesis of COVID-19, we used mice deficient in C7 ($C7^{-/-}$), a key component of MAC formation that does not affect the generation of upstream biologically active complement activation products [47]. $C7^{-/-}$ and $C7^{+/+}$ mice were intranasally inoculated with a sublethal dose of MA30 (2.5×10^4 $TCID_{50}$). Both male and female $C7^{-/-}$ mice had a lower percent body weight loss with a similar viral sub genomic load and viral S protein staining in the lungs as compared with the $C7^{+/+}$ counterparts within 7 DPI (Fig. 5A-B and S6A-B). Sera collected from infected $C7^{-/-}$ mice lacked complement-mediated hemolytic activity, unlike sera from infected $C7^{+/+}$ mice (Fig. 5C), confirming insufficiency of MAC formation in $C7^{-/-}$ serum. There were no significant differences in
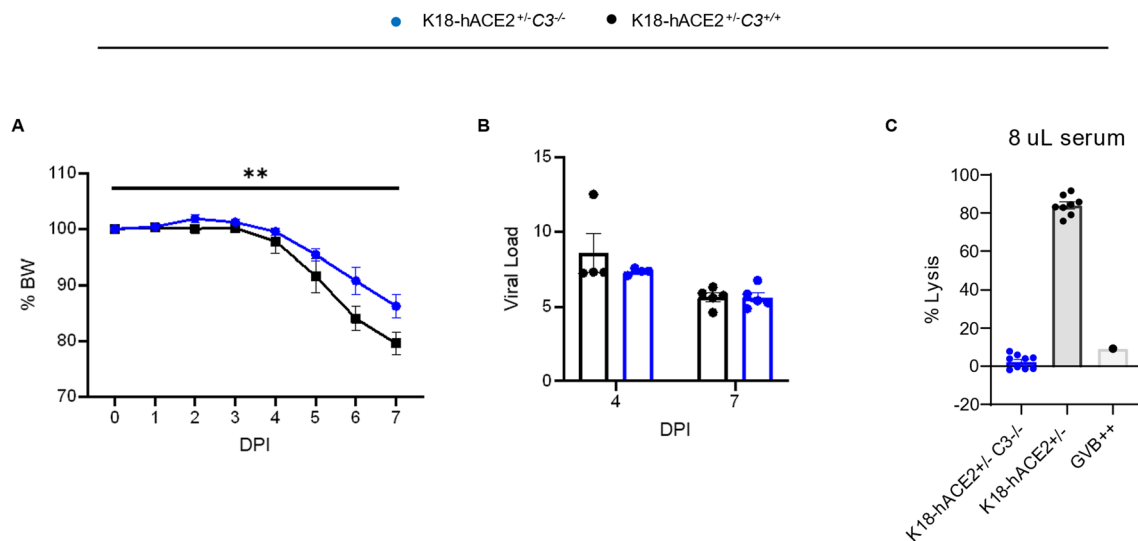
Fig. 3 Deficiency of C3 protects against severe COVID-19 in K18-hACE2 transgenic mice infected with an original SARS-CoV2 strain. **A–C** C3 deficient and sufficient mice expressing hACE2 under the control of the K18 promoter ($C3^{-/-}/K18$-$hACE2^{+/-}$ and $C3^{+/+}/K18$-$hACE2^{+/-}$) aged 15 weeks with mixed-sex were infected with SARS-CoV-2-WA1 strain ($n = 9$/group, 5 females and 4 males per group) with 4 mice/group euthanized at 4 DPI and the others at 7 DPI. **A** Percent body weight changes. p-value = 0.0036 by two-way ANOVA, and **B** viral load of lung by qPCR showing no significance after infection. **C** Hemolytic activity of the infected $C3^{-/-}/K18$-$hACE2^{+/-}$ and $C3^{+/+}/K18$-$hACE2^{+/-}$ at 3 and 7 DPI using 8% diluted serum as the source of complement

serum C3a and C5a levels between infected $C7^{-/-}$ and $C7^{+/+}$ mice, consistent with the downstream position of C7 in the complement activation pathway (Fig. 5D-E). These results indicate that during infection, early complement activation is independent of C7 gene expression. Histologically, we found that infected $C7^{-/-}$ mice had less pulmonary edema than infected $C7^{+/+}$ mice (Fig. 5F-G); whereas bronchial epithelial degeneration and interstitial inflammatory cell infiltrates were similar between these two groups (Figure S5). Thus, C7 deficiency specifically preventing MAC formation protects against severe COVID-19. This result, together with the above data with $Cd59ab^{-/-}$ mice, indicates MAC-specific acceleration of severe COVID-19.

To investigate the cellular mechanism underlying MAC-accelerated severe COVID19, we measured serum levels of vWF (Von Willebrand Factor) and VEGF (vascular endothelial growth factor), established biomarkers for monitoring endothelial dysfunction [55, 72]. We found that infected $C7^{+/+}$ mice had significantly higher levels of both vWF and VEGF compared to infected $C7^{-/-}$ mice, at both 4 and 7 DPI (Fig. 5H-I), indicating that MAC contributes to COVID-19 pathogenesis by causing endothelial dysfunction/activation.

Infected C3$^{-/-}$ and C7$^{-/-}$ mice had decreased, and Cd59ab$^{-/-}$ mice had increased, MAC deposition in the lungs

To directly monitor the impact of complement modulation in the above experimental paradigms, we stained for MAC and C3 deposition in infected lungs. Infected B6 mice had significantly higher levels of MAC (Figure S7) and C3 deposition (Figure S8) in pulmonary tissues compared to naïve B6 mice. Infected $Cd59ab^{-/-}$ mice had increased levels of MAC and C3 deposition (Figs. 6A-B and Figure S7) and $C3^{-/-}$ mice had reduced MAC and lack of C3 deposition in pulmonary tissues and cells compared to infected control mice (Figs. 7A-B and S8). Notably, deficiency of C7 resulted in reduced MAC but enhanced C3 deposition in pulmonary tissue and cells (Figs. 7C-D and Figure S8). Thus, C3 and C7 deficiency results in decreased MAC deposition in the lungs of infected mice, whereas CD59 deficiency results in increased MAC deposition.

Discussion

In this paper, we document that mice infected with a sublethal dose of MA30, a mouse-adapted SARS-CoV-2 strain, had sustained ongoing systemic serum complement activation during the acute phase of infection. This was evidenced by increased serum levels of C3a and C5a and a reduced capacity of mouse serum to mediate MAC-induced hemolysis. We also found that there were continuously increased C3a and C5a levels in infected mouse sera from 0 to 7 DPI (Fig. 1B and C), indicating sustained ongoing complement activation during acute MA30 infection. These results are consistent with clinical findings that severe COVID-19 patients have persistently increased levels of soluble MAC,
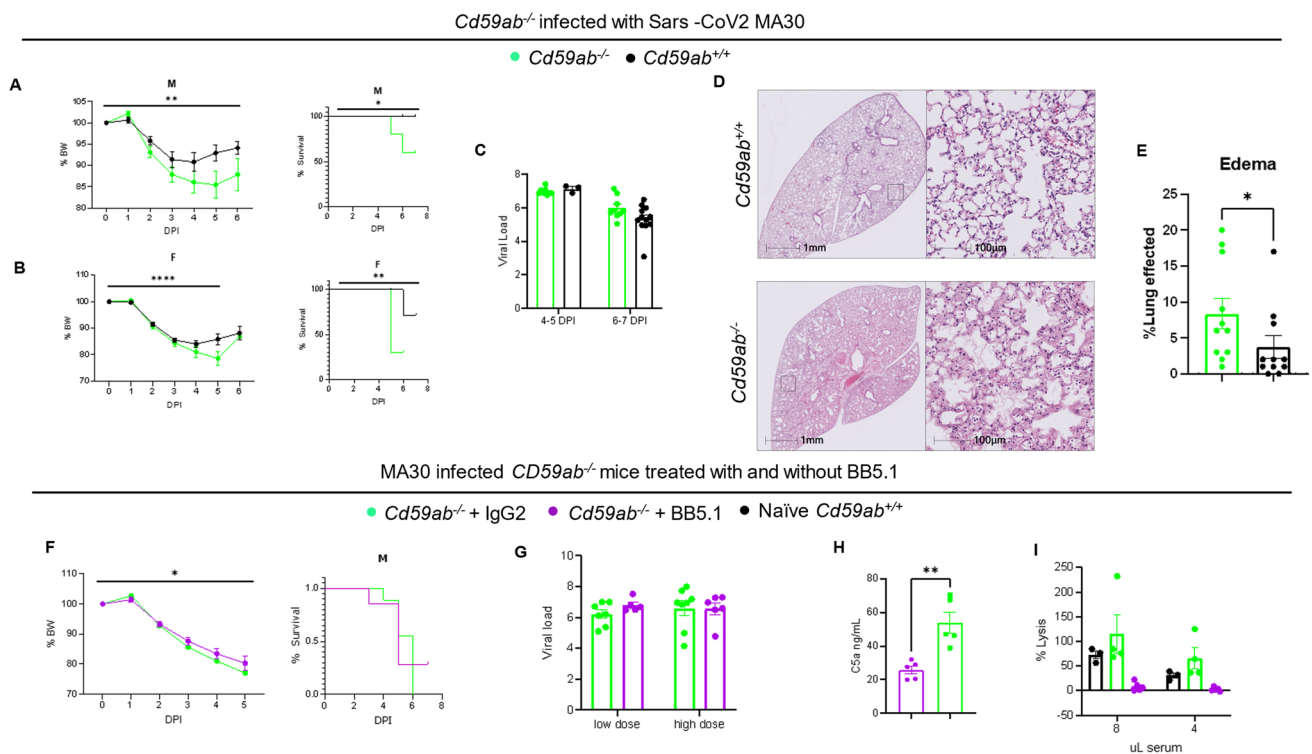
Fig. 4 Increase and reduction in MAC formation accelerates or partially rescues severe COVID-19, respectively. Administration of an anti-C5 inhibitor BB5.1 partially rescues the deleterious effects of CD59 deficiency. **A–E** $Cd59ab^{-/-}$ ($n=10$ males, $n=10$ females) and $Cd59ab^{+/+}$ mice ($n=10$ males, $n=10$ females) were age-matched at 16-20 week old and infected with a sublethal dose of MA30 SARS-CoV2 of 1×10^4 TCID$_{50}$. Percent body weight changes and survival of **A** male mice and **B** female mice after infection. **C** Viral load showed no significant difference. **D** Representative images of lung H/E sec-tions from $Cd59ab$ sufficient and deficient groups with **E** quantifica-tion thereof. **F–I** $Cd59ab^{-/-}$ mice were infected with sublethal doses (1 and 2.5×10^4 TCID$_{50}$) of MA30 SARS-CoV-2 and treated with control isotype IgG ($n=12$) or anti-C5 BB5.1 antibody ($n=16$). **F** Per-cent body weight changes and survival in infected males ($n=9$/group). **G** Viral load in the lungs showing no significance with unpaired t-tests. **H** C5a levels in the sera after infection, significance from unpaired t-test. **I** Complement activity as measured by hemolytic assay of the infected mice sera at serial dilution

C3a and C5a in their serum [24, 34–39]. We also found that C3a but not C5a levels in serum were increased in infected males compared with infected females (Figure S1). This result is consistent with the previous finding that C3 activity was increased in male B6 mice after intestinal ischemic reperfusion injury or via activation of the classical pathway [73, 74]. Further, scRNA-seq of the infected mouse lung revealed an up-regulation of the transcripts of several com-plement genes (*C1qa*, *C1qb*, *C1qc*, *C4a*, *C4b*, *C2*, *C3* and *Cfb*) in myeloid cells and endothelial cells of MA30-infected lungs. Our previous study in the well-established SARS-CoV-2-WA1-infected K18-hACE2 model, showed upregu-lation of complement pathways in the lungs and upregula-tion of complement genes such as *C1qa*, *C1qb* and *Cfb* in myeloid cells and fibroblast cells of infected mice at 4, 6 [32], and even 21 DPI [75]. This local upregulation may contribute to ongoing complement activation by comple-ment products synthesized locally by tissue-resident cells, rather than by liver-derived systemic production [1]. Previ-ous studies have implicated complement upregulation as a

risk factor for 60-day mortality in COVID-19 patients [24]. Whether the increased local production of these comple-ment components in these immune cells also contribute to the ongoing complement activation, leading to accelerated severe COVID-19 seen in patients, remains unclear and war-rants further investigation [1].

Our study has defined a causative effect of MAC in accel-erating severe COVID-19 by both gain- and loss-of-function approaches. The lack of total complement activation due to deficiency of C3 in both B6 and K18-hACE2 compound backgrounds protected against severe diseases following infection by a lethal dose (LD$_{75}$) of MA30 and a sublethal dose of SARS-CoV-2-WA1 strain, respectively. Abrogation of MAC formation due to C7 deficiency attenuated while enhanced MAC formation due to CD59 deficiency acceler-ated severe COVID-19. Further, therapeutic inhibition of MAC formation with BB5.1 antibody treatment partially protected against the development of severe COVID-19 in CD59 deficient mice. The protective and harmful effects seen in these deficient mice were independent of viral load.
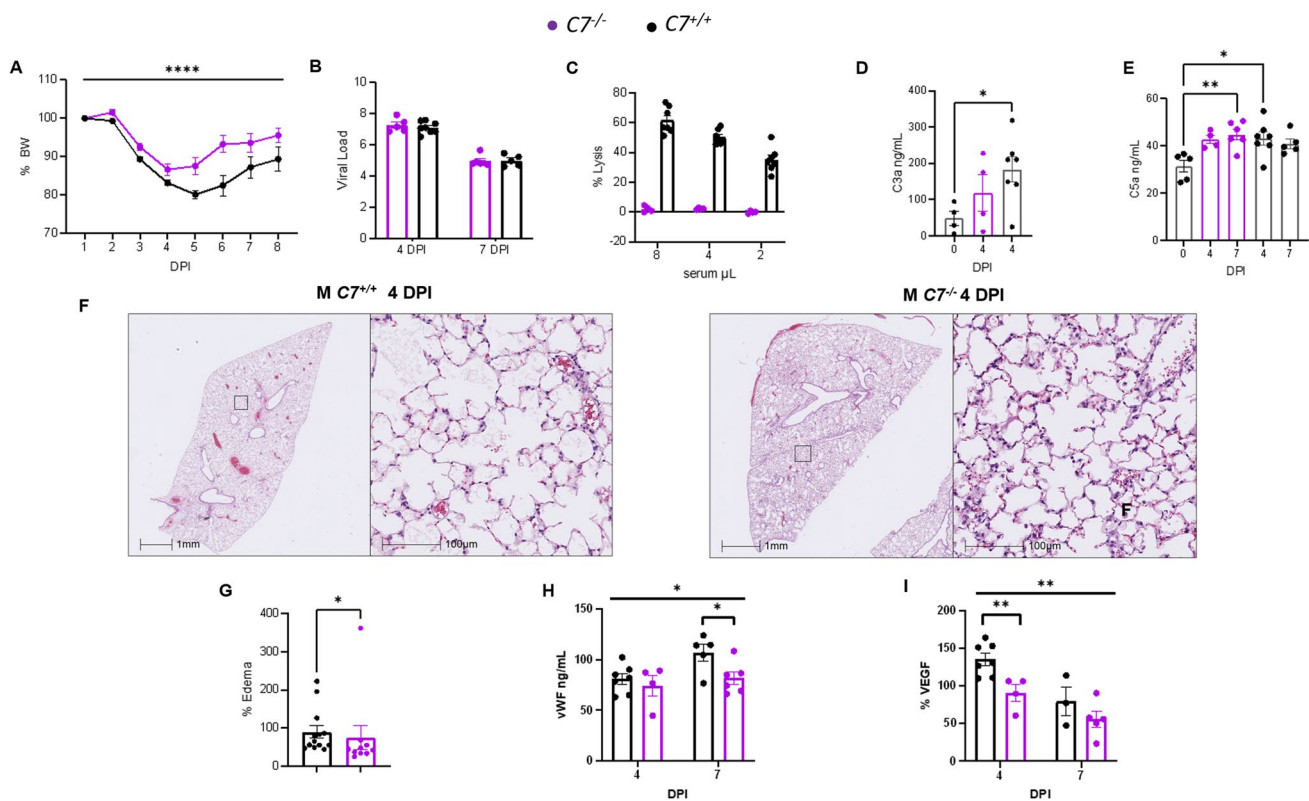
Fig. 5 Deficiency of C7 protects against severe COVID-19. **A–I** Mixed sex $C7^{+/+}$ ($n = 14$, 10 males, 4 females) and $C7^{-/-}$ mice ($n=11$, 7 males, 4 females) aged 15–17 weeks were infected with an infectious dose of MA30 SARS-CoV-2 (2.5×10^4 $TCID_{50}$) and euthanized at 4 and 7 DPI. **A** Percent body weight changes as assessed by Two-way ANOVA. **B** viral load after infection as measured by qPCR. **C** Hemolytic assay showing complement activity as measured by serial dilution of the infected sera as a source of the complement to lyse the anti-body sensitized sheep erythrocytes. **D-E** C3a (**D**) and C5a (**E**) measurements of the sera from the infected mice by ELISA with significant differences as assessed by One-way ANOVA with Dunnet's (**D**) or Tukey's (**E**) multiple comparisons. **F-G** Representative images of pulmonary edema at 4 DPI (**F**) and quantification (**G**) analyzed by Student t-test. **H-I** vWF (**H**) and VEGF (**I**) serum levels (ng/mL) at 4 and 7 DPI. Overall signficiance assessed by One-way ANOVA and indicated by horizontal bar with individual comparisons assessed by two-tailed Student t-test. * $p < 0.05$, ** $p < 0.01$, **** $p < 0.0001$

This is in line with the clinical observation that heightened complement activation is associated with COVID-19 [24, 34–39], SARS, and MERS [1, 76, 77]. A previous study using a different viral strain than that used here also showed that $C3^{-/-}$ mice were protected from SARS-CoV [78]. Mouse-adapted SARS-CoV-infected $C3^{-/-}$ mice did not have any weight loss after the infection, and respiratory function was improved compared to the infected controls [78]. A similar observation was found in our study with MA30-infected B6 mice. The infected $C3^{-/-}$ mice, when challenged with the LD_{75} of MA30, exhibited significantly improved survival, minimal weight loss, and reduced pulmonary edema compared to infected control $C3^{+/+}$ mice. It is important to know that increase in body weight loss and mortality rate associated with the rapid development of pulmonary edema are the typical features of the severe diseases phenotypes seen in MA30-infected B6 mice [58]. To our knowledge, there are no previous studies that utilize complement-deficient mice to dissect the role of specific complement pathways

or complement components in the pathogenesis of severe COVID-19[1], and our results document a critical pathogenic role for the MAC in severe COVID-19.

Early clinical observations showed that there were heightened C3 and C5b-9 deposits on lung endothelium and increased C5a in bronchoalveolar lavage fluid (BALF) [27, 37, 40]. However, these studies did not directly examine the consequence of MAC deposition on the pathogenesis and disease severity as observed in patients. Here, we showed that there was decreased MAC deposition in the lungs of infected $C3^{-/-}$ and $C7^{-/-}$ mice, and increased MAC deposition in the lungs of $Cd59ab^{-/-}$ mice as compared to their respective control mice. The level of MAC deposition on alveoli, epithelial cells, and endothelial cells in the various complement-deficient mice correlated with disease severity, pathological changes, and survival. However, C3 deposits in the lungs of these infected mice did not show the same trend. One of the major pathological changes seen in severe COVID-19 patients is alveolar edema [79–84]. Consistently,
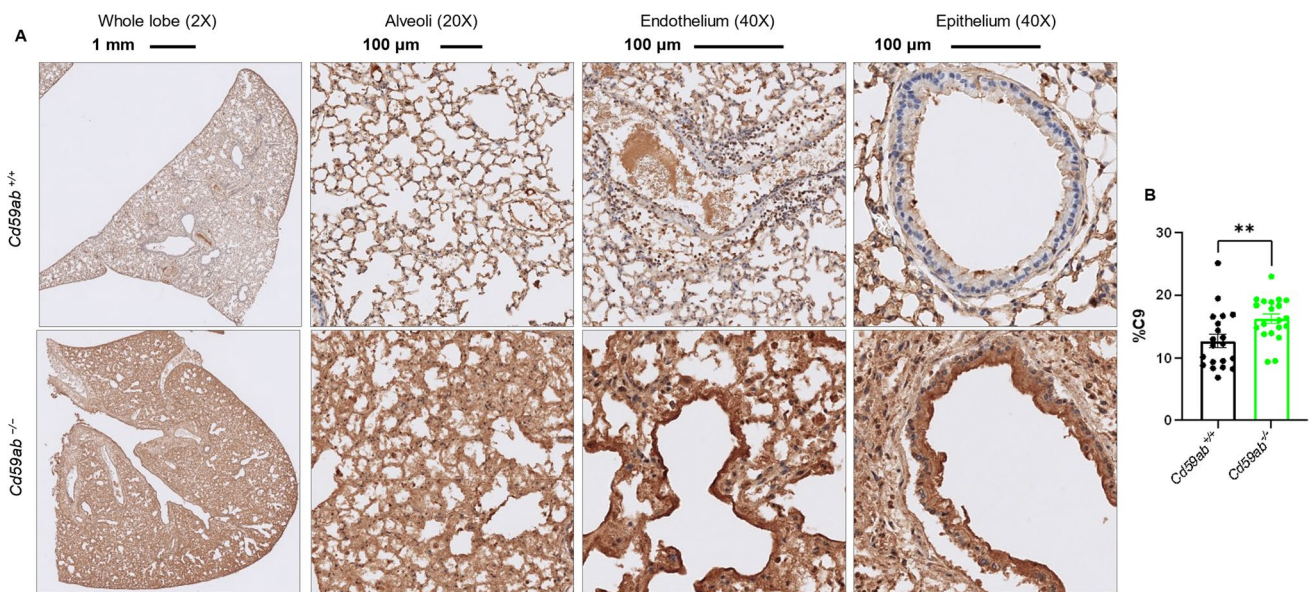
Fig. 6 MAC deposition in the lungs of *Cd59ab^-/-* mice as assessed by C9 staining. **A-B** Age-matched 16-20 week-old male and female *Cd59ab^{-/-}* and control *Cd59ab^{+/+}* mice were sacrificed and tissues collected after death at 4-7 DPI after infection with MA30 (1×10^4 TCID$_{50}$). MAC deposition was viewed by staining with polyclonal rabbit anti-rat C9 (kindly obtained from Dr. Paul Morgan) at a 1:400 dilution. **A** Representative images of the above groups at 5 DPI showing whole lung lobe at magnification 2X, Alveoli at 20X, and epithelium and endothelium at 40X. **B** Quantification of C9. ** $p < 0.01$ by two-tailed Student's *t*-test

our data showed that decreased MAC deposits were associated with reduced while increased MAC deposits were associated with more edema in the lungs of our experimental mice. Further, the lack of terminal complement activation and formation of the MAC in C7 deficient mice protected against endothelial dysfunction, which was associated with the attenuation of pulmonary edema and disease.

In summary, these results indicate an important pathogenic role for the MAC in severe COVID-19. However, the molecular and cellular mechanisms underlying MAC-accelerated severe COVID-19 remain unclear. Previous studies have elucidated a mechanism by which MAC forms sublytic pores and subsequent ion influx in nucleated cells resulting in the release of inflammatory cytokines such as basic fibroblast growth factor and platelet-derived growth factor, which may contribute to the pathogenesis of complement-mediated diseases [9, 21, 85]. However, the pathological role of sublytic MAC in the severe COVID-19 remains unclear and warrants further investigation. Our results also show that systemic inhibition of MAC formation by C3 or C7 deficiency does not increase viral load in SARS-CoV2 infection (Figs. 1, 2 and 4). This result suggests that SARS-CoV2 possesses a strategy to evade MAC-mediated virolysis and complement opsonization. SARS-CoV-2 has been implicated in employing several immune evasion mechanisms to avoid host attack via autophagy flux disruption and blockage [86, 87] as well as the weak binding ability of Omicron with HLA class I polymorphisms [88]. RRV and HIV utilize multiple mechanisms to escape complement attack, such as the recruitment of factor H, CD59 or CD55 to the membrane. Whether SARS-CoV2, a respiratory virus, possesses similar mechanisms for complement evasion remains unknown. A recent study shows that SARS-CoV-2-encoded ORF8 protein may contribute to the decay of C3-convertase to inhibit complement activation [89]. However, how this mechanism and other evasion mechanisms contribute to MAC-accelerated COVID-19 requires further investigation. Moreover, it is not completely understood how, and which complement pathways are activated in SARS-CoV-2 infection, and what their relative roles are in COVID-19. From a clinical standpoint, we show that a murine form of eculizumab provides a partial protective effect against severe COVID-19 in CD59 deficient mice and inhibits the formation of MAC, as determined by measurement of soluble MAC in circulation. However, it remains to be determined whether the dosing regimen we used is sufficient to block the formation of MAC in the lungs after the infection. Therefore, future studies with additional dose ranges and duration are needed to further test the therapeutic value of anti-MAC for treatment of severe COVID-19. Of note, eculizumab showed limited beneficial effects in clinical trials [90–94]. A thorough dissection of these questions may provide therapeutic targets and build a strong foundation to protect against future pandemics.
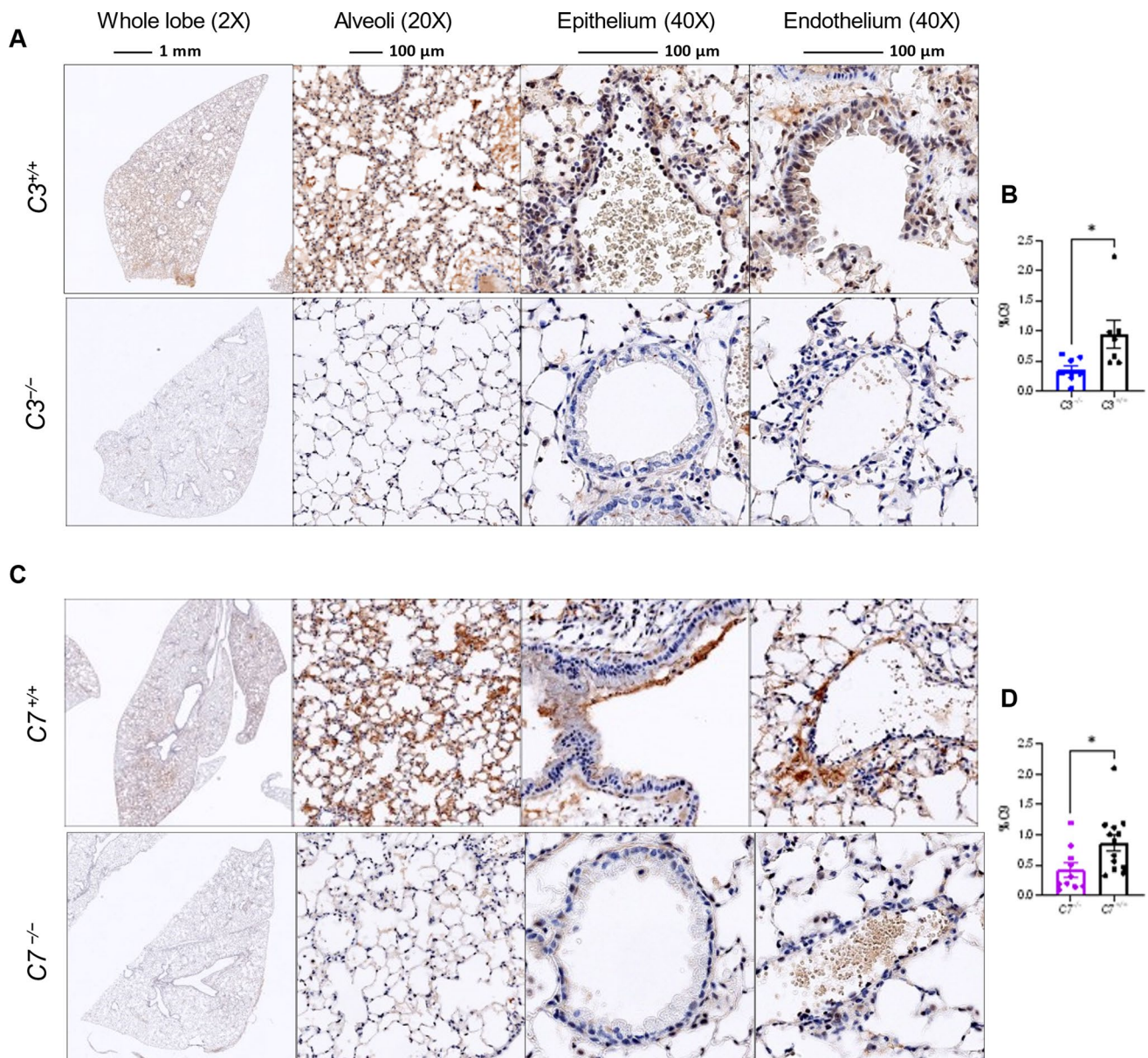
Fig. 7 MAC deposition in the lungs as assessed by C9 staining. **A–D** Mouse lung sections were stained with an antibody against C9 (USBiological Life Sciences, 362359, Rabbit Anti-C9) used at a 1:1000 dilution. Representative images of the above groups showing whole lung lobe at magnification 2X, Alveoli at 20X, and epithelium and endothelium at 40X. **A** Representative image at 3DPI of lungs of C3 deficient and sufficient mice which were infected with MA30 at a dose of 5×104 TCID50, and **B** quantification of C9 staining. **C** Representative image at 4DPI of lungs of C7 deficient and sufficient mice which were were infected with a dose of MA30 $2.5×10^4$ TCID50, and **D** quantification of C9 staining. *$p < 0.05$ by two-tailed Student *t*-test

Data availability The data that support the findings of this study are available from the corresponding author upon reasonable request.

Declarations

Conflict of interest The authors have declared that no conflict of interest exists.

Ethical approval Our research follows Tulane University's Institutional Animal Care and Use Committee-approved protocols (1557 and 1331) and complied with all relevant ethical regulations for animal treatment.

References

1. Xiao MT, Ellsworth CR, Qin X (2024) Emerging role of complement in COVID-19 and other respiratory virus diseases. Cell Mol Life Sci 81(1):94

2. Yan B, Freiwald T, Chauss D, Wang L, West E, Mirabelli C et al (2021) SARS-CoV-2 drives JAK1/2-dependent local complement hyperactivation. Sci Immunol. https://doi.org/10.1126/sciimmunol.abg0833

3. Hess C, Kemper C (2016) Complement-mediated regulation of metabolism and basic cellular processes. Immunity 45(2):240–254

4. Van Damme KFA, Hoste L, Declercq J, De Leeuw E, Maes B, Martens L et al (2023) A complement atlas identifies interleukin-6-dependent alternative pathway dysregulation as a key druggable feature of COVID-19. Sci Transl Med 15(710):eadi0252

5. Qin X, Gao B (2006) The complement system in liver diseases. Cell Mol Immunol 3(5):333–340

6. Zhou X, Hu W, Qin X (2008) The role of complement in the mechanism of action of rituximab for B-cell lymphoma: implications for therapy. Oncologist 13(9):954–966

7. Morgan BP, Harris CL (1999) Complement regulatory proteins. Academic Press, London

8. Qin X, Goldfine A, Krumrei N, Grubissich L, Acosta J, Chorev M et al (2004) Glycation inactivation of the complement regulatory protein CD59: a possible role in the pathogenesis of the vascular complications of human diabetes. Diabetes 53(10):2653–2661

9. Acosta J, Qin X, Halperin J (2004) Complement and complement regulatory proteins as potential molecular targets for vascular diseases. Curr Pharm Des 10(2):203–211

10. Walport MJ (2001) Complement. First of two parts. N Engl J Med 344(14):1058–66

11. Walport MJ (2001) Complement. Second of two parts. N Engl J Med 344(15):1140–4

12. Carney DF, Lang TJ, Shin ML (1990) Multiple signal messengers generated by terminal complement complexes and their role in terminal complexes elimination. J Immunol 145:621–629

13. Papadimitriou JC, Ramm LE, Drachenberg CB, Trump BF, Shin ML (1991) Quantitative analysis of adenine nucleotides during the prelytic phase of cell death mediated by C5b–9. J Immunol 147(1):212–217

14. Niculescu F, Rus H, van Biesen T, Shin ML (1997) Activation of Ras and mitogen-activated protein kinase pathway by terminal complement complexes is G protein dependent. J Immunol 158(9):4405–4412

15. Niculescu F, Rus H (1999) Complement activation and atherosclerosis. Mol Immunol 36(13–14):949–955

16. Niculescu F, Badea T, Rus H (1999) Sublytic C5b–9 induces proliferation of human aortic smooth muscle cells: role of mitogen activated protein kinase and phosphatidylinositol 3-kinase. Atherosclerosis 142(1):47–56

17. Niculescu F, Rus H (2004) The role of complement activation in atherosclerosis. Immunol Res 30(1):73–80

18. Hila S, Soane L, Koski CL (2001) Sublytic C5b-9-stimulated Schwann cell survival through PI 3-kinase-mediated phosphorylation of BAD. Glia 36(1):58–67

19. Soane L, Cho HJ, Niculescu F, Rus H, Shin ML (2001) C5b–9 terminal complement complex protects oligodendrocytes from death by regulating Bad through phosphatidylinositol 3-kinase/Akt pathway. J Immunol 167(4):2305–2311

20. Fosbrink M, Niculescu F, Rus V, Shin ML, Rus H (2006) C5b-9-induced endothelial cell proliferation and migration are dependent on Akt inactivation of forkhead transcription factor FOXO1. J Biol Chem 281(28):19009–19018

21. Benzaquen LR, Nicholson-Weller A, Halperin JA (1994) Terminal complement proteins C5b–9 release basic fibroblast growth factor and platelet-derived growth factor from endothelial cells. J Exp Med 179(3):985–992

22. Nicholson-Weller A, Halperin JA (1993) Membrane signaling by complement C5b–9, the membrane attack complex. Immunol Res 12(3):244–257

23. Sugita Y, Tobe T, Oda E, Tomita M, Yasukawa K, Yamaji N et al (1989) Molecular cloning and characterization of MACIF, an inhibitor of membrane channel formation of complement. J Biochem (Tokyo) 106(4):555–557

24. Barratt-Due A, Pettersen K, Børresdatter-Dahl T, Holter JC, Grønli RH, Dyrhol-Riise AM et al (2024) Escalated complement activation during hospitalization is associated with higher risk of 60-day mortality in SARS-CoV-2-infected patients. J Intern Med. https://doi.org/10.1111/joim.13783

25. Stenmark KR, Frid MG, Gerasimovskaya E, Zhang H, McCarthy MK, Thurman JM et al (2021) Mechanisms of SARS-CoV-2-induced lung vascular disease: potential role of complement. Pulm Circ 11(2):20458940211015800

26. Yu J, Yuan X, Chen H, Chaturvedi S, Braunstein EM, Brodsky RA (2020) Direct activation of the alternative complement pathway

by SARS-CoV-2 spike proteins is blocked by factor D inhibition. Blood 136(18):2080–2089

27. Skendros P, Mitsios A, Chrysanthopoulou A, Mastellos DC, Metallidis S, Rafailidis P et al (2020) Complement and tissue factor-enriched neutrophil extracellular traps are key drivers in COVID-19 immunothrombosis. J Clin Invest 130(11):6151–6157

28. Chouaki Benmansour N, Carvelli J, Vivier E (2021) Complement cascade in severe forms of COVID-19: recent advances in therapy. Eur J Immunol 51(7):1652–1659

29. de Nooijer AH, Grondman I, Janssen NAF, Netea MG, Willems L, van de Veerdonk FL et al (2021) Complement activation in the disease course of coronavirus disease 2019 and its effects on clinical outcomes. J Infect Dis 223(2):214–224

30. Carvelli J, Demaria O, Vely F, Batista L, Chouaki Benmansour N, Fares J et al (2020) Association of COVID-19 inflammation with activation of the C5a–C5aR1 axis. Nature 588(7836):146–150

31. Ma L, Sahu SK, Cano M, Kuppuswamy V, Bajwa J, McPhatter J et al (2021) Increased complement activation is a distinctive feature of severe SARS-CoV-2 infection. Sci Immunol. https://doi.org/10.1126/sciimmunol.abh2259

32. Qin Z, Liu F, Blair R, Wang C, Yang H, Mudd J et al (2021) Endothelial cell infection and dysfunction, immune activation in severe COVID-19. Theranostics 11(16):8076–8091

33. Liu F, Han K, Blair R, Kenst K, Qin Z, Upcin B et al (2021) SARS-CoV-2 infects endothelial cells in vivo and in vitro. Front Cell Infect Microbiol 11:701278

34. Peffault de Latour R, Bergeron A, Lengline E, Dupont T, Marchal A, Galicier L et al (2020) Complement C5 inhibition in patients with COVID-19 - a promising target? Haematologica 105(12):2847–50

35. Holter JC, Pischke SE, de Boer E, Lind A, Jenum S, Holten AR et al (2020) Systemic complement activation is associated with respiratory failure in COVID-19 hospitalized patients. Proc Natl Acad Sci 117(40):25018–25025

36. Sinkovits G, Mező B, Réti M, Müller V, Iványi Z, Gál J et al (2021) Complement overactivation and consumption predicts in-hospital mortality in SARS-CoV-2 infection. Front Immunol 12:663187

37. Carvelli J, Demaria O, Vély F, Batista L, Chouaki Benmansour N, Fares J et al (2020) Association of COVID-19 inflammation with activation of the C5a–C5aR1 axis. Nature 588(7836):146–150

38. Rajamanickam A, Nathella PK, Venkataraman A, Dasan B, Putlibai S, Ahamed SF et al (2023) Levels of complement components in children with acute COVID-19 or multisystem inflammatory syndrome. JAMA Network Open 6(3):e231713-e

39. Savitt AG, Manimala S, White T, Fandaros M, Yin W, Duan H et al (2021) SARS-CoV-2 exacerbates COVID-19 pathology through activation of the complement and kinin systems. Front Immunol 12:767347

40. Macor P, Durigutto P, Mangogna A, Bussani R, De Maso L, D'Errico S et al (2021) Multiple-organ complement deposition on vascular endothelium in COVID-19 patients. Biomedicines 9(8):1003

41. Lo MW, Kemper C, Woodruff TM (2020) COVID-19: complement, coagulation, and collateral damage. J Immunol 205(6):1488–1495

42. Morrison TE, Fraser RJ, Smith PN, Mahalingam S, Heise MT (2007) Complement contributes to inflammatory tissue destruction in a mouse model of Ross River virus-induced disease. J Virol 81(10):5132–5143

43. Stoiber H, Speth C, Dierich MP (2003) Role of complement in the control of HIV dynamics and pathogenesis. Vaccine 21:S77–S82

44. Liu F, Dai S, Gordon J, Qin X (2014) Complement and HIV-I infection/HIV-associated neurocognitive disorders. J Neurovirol 20(2):184–198

45. Soederholm A, Bánki Z, Wilflingseder D, Gassner C, Zwirner J, López-Trascasa M et al (2007) HIV-1 induced generation of C5a attracts immature dendritic cells and promotes infection of autologous T cells. Eur J Immunol 37(8):2156–2163

46. Stoiber H, Frank I, Spruth M, Schwendinger M, Mullauer B, Windisch JM et al (1997) Inhibiton of HIV-1 infection in vitro by monoclonal antibodies to the complement receptor type 3 (CR3): an accessory role for CR3 during virus entry? Mol Immunol 34(12):855–863

47. Yu Q, Yu R, Qin X (2010) The good and evil of complement activation in HIV-1 infection. Cell Mol Immunol 7(5):334–340

48. Montefiori DC, Cornell RJ, Zhou JY, Zhou JT, Hirsch VM, Johnson PR (1994) Complement control proteins, CD46, CD55, and CD59, as common surface constituents of human and simian immunodeficiency viruses and possible targets for vaccine protection. Virology 205(1):82–92

49. Ruggenenti P, Di Marco F, Cortinovis M, Lorini L, Sala S, Novelli L et al (2021) Eculizumab in patients with severe coronavirus disease 2019 (COVID-19) requiring continuous positive airway pressure ventilator support: retrospective cohort study. PLoS One 16(12):e0261113

50. Annane D, Heming N, Grimaldi-Bensouda L, Frémeaux-Bacchi V, Vigan M, Roux A-L et al (2020) Eculizumab as an emergency treatment for adult patients with severe COVID-19 in the intensive care unit: a proof-of-concept study. EClinicalMedicine 28:100590

51. Witzenrath M, Paassen P, Heunks L, Mourvillier B, de Bruin S, Lim E et al (2022) Anti-C5a antibody (vilobelimab) therapy for critically ill, invasively mechanically ventilated patients with COVID-19 (PANAMO): a multicentre, double-blind, randomised, placebo-controlled, phase 3 trial. Lancet Respir Med 10:1137–1146

52. Skendros P, Germanidis G, Mastellos DC, Antoniadou C, Gavriilidis E, Kalopitas G et al (2022) Complement C3 inhibition in severe COVID-19 using compstatin AMY-101. Sci Adv 8(33):eabo2341

53. Qin X, Hu W, Song W, Grubissich L, Hu X, Wu G et al (2009) Generation and phenotyping of mCd59a and mCd59b double-knockout mice. Am J Hematol 84(2):65–70

54. Qin X, Hu W, Song W, Blair P, Wu G, Hu X et al (2009) Balancing role of nitric oxide in complement-mediated activation of platelets from mCd59a and mCd59b double-knockout mice. Am J Hematol 84(4):221–227

55. Wu G, Hu W, Shahsafaei A, Song W, Dobarro M, Sukhova GK et al (2009) Complement regulator CD59 protects against atherosclerosis by restricting the formation of complement membrane attack complex. Circ Res 104(4):550–558

56. Wu G, Chen T, Shahsafaei A, Hu W, Bronson RT, Shi GP et al (2010) Complement regulator CD59 protects against angiotensin II-induced abdominal aortic aneurysms in mice. Circulation 121(11):1338–1346

57. Wong L-YR, Zheng J, Wilhelmsen K, Li K, Ortiz ME, Schnicker NJ et al (2022) Eicosanoid signalling blockade protects middle-aged mice from severe COVID-19. Nature 605(7908):146–51

58. Ellsworth CR, Wang C, Katz AR, Chen Z, Islamuddin M, Yang H et al (2024) Natural killer cells do not attenuate a mouse-adapted SARS-CoV-2-induced disease in rag2−/− mice. Viruses 16(4):611

59. Han K, Blair RV, Iwanaga N, Liu F, Russell-Lodrigue KE, Qin Z et al (2021) Lung expression of human angiotensin-converting enzyme 2 sensitizes the mouse to SARS-CoV-2 infection. Am J Respir Cell Mol Biol 64(1):79–88

60. Ramaglia V, King RH, Nourallah M, Wolterman R, de Jonge R, Ramkema M et al (2007) The membrane attack complex of the complement system is essential for rapid Wallerian degeneration. J Neurosci 27(29):7663–7672

61. Götz P, Azubuike-Osu SO, Braumandl A, Arnholdt C, Kübler M, Richter L et al (2022) Cobra venom factor boosts arteriogenesis in mice. Int J Mol Sci. 23(15):8454

62. Wang C, Khatun MS, Zhang Z, Allen MJ, Chen Z, Ellsworth CR et al (2023) COVID-19 and influenza infections mediate distinct pulmonary cellular and transcriptomic changes. Commun Biol 6(1):1265

63. Wang C, Khatun MS, Ellsworth CR, Chen Z, Islamuddin M, Nisperuza Vidal AK, Alam MA, Liu S, Mccombs JE, Maness NJ, Blair RV, Kolls JK, Qin X (2024) Deficiency of Tlr7 and Irf7 in mice increases the severity of COVID-19 through the reduced interferon production. Commun Biol. In press

64. Powell MB, Marchbank KJ, Rushmere NK, van den Berg CW, Morgan BP (1997) Molecular cloning, chromosomal localization, expression, and functional characterization of the mouse analogue of human CD59. J Immunol 158:1692–1702

65. Qian YM, Qin X, Miwa T, Sun X, Halperin JA, Song WC (2000) Identification and functional characterization of a new gene encoding the mouse terminal complement inhibitor CD59. J Immunol 165(5):2528–2534

66. Baalasubramanian S, Harris CL, Donev RM, Mizuno M, Omidvar N, Song WC et al (2004) CD59a is the primary regulator of membrane attack complex assembly in the mouse. J Immunol 173(6):3684–3692

67. Qin X, Dobarro M, Bedford SJ, Ferris S, Miranda PV, Song W et al (2005) Further characterization of reproductive abnormalities in mCd59b knockout mice: a potential new function of mCd59 in male reproduction. J Immunol 175(10):6294–6302

68. Qin X, Miwa T, Aktas H, Gao M, Lee C, Qian YM et al (2001) Genomic structure, functional comparison, and tissue distribution of mouse Cd59a and Cd59b. Mamm Genome 12(8):582–589

69. Qin X, Dobarro M, Bedford SJ, Ferris S, Miranda PV, Song W et al (2005) Further characterization of reproductive abnormalities in mCd59b knockout mice: a potential new function of mCd59 in male reproduction1. J Immunol 175(10):6294–6302

70. Qin X, Ferris S, Hu W, Guo F, Ziegeler G, Halperin JA (2006) Analysis of the promoters and 5'-UTR of mouse Cd59 genes, and of their functional activity in erythrocytes. Genes Immun 7(4):287–297

71. Al-Ani F, Chin-Yee I, Lazo-Langner A (2016) Eculizumab in the management of paroxysmal nocturnal hemoglobinuria: patient selection and special considerations. Ther Clin Risk Manag 12:1161–1170

72. Mohebbi A, Haybar H, Nakhaei Moghaddam F, Rasti Z, Vahid MA, Saki N (2023) Biomarkers of endothelial dysfunction are associated with poor outcome in COVID-19 patients: a systematic review and meta-analysis. Rev Med Virol 33(4):e2442

73. Kotimaa J, Klar-Mohammad N, Gueler F, Schilders G, Jansen A, Rutjes H et al (2016) Sex matters: systemic complement activity of female C57BL/6J and BALB/cJ mice is limited by serum terminal pathway components. Mol Immunol 76:13–21

74. Wu M, Rowe JM, Fleming SD (2021) Complement initiation varies by sex in intestinal ischemia reperfusion injury. Front Immunol 12:649882

75. Wang C, Khatun MS, Zhang Z, Allen MJ, Chen Z, Ellsworth CR et al (2023) COVID-19 and influenza infections mediate distinct pulmonary cellular and transcriptomic changes. Commun Biol 6(1):1265

76. Zhou Y, Lu K, Pfefferle S, Bertram S, Glowacka I, Drosten C et al (2010) A Single Asparagine-linked glycosylation site of the severe acute respiratory syndrome coronavirus spike glycoprotein facilitates inhibition by mannose-binding lectin through multiple mechanisms. J Virol 84(17):8753–8764

77. Hamed ME, Naeem A, Alkadi H, Alamri AA, AlYami AS, AlJurryyan A et al (2021) Elevated expression levels of lung complement anaphylatoxin, neutrophil chemoattractant chemokine IL-8, and RANTES in MERS-CoV-infected patients: predictive biomarkers for disease severity and mortality. J Clin Immunol 41(7):1607–1620

78. Gralinski LE, Sheahan TP, Morrison TE, Menachery VD, Jensen K, Leist SR et al (2018) Complement activation contributes to severe acute respiratory syndrome coronavirus pathogenesis. mBio https://doi.org/10.1128/mBio.01753-18

79. Liu J, Li Y, Liu Q, Yao Q, Wang X, Zhang H et al (2021) SARS-CoV-2 cell tropism and multiorgan infection. Cell Discov 7(1):17

80. Bösmüller H, Matter M, Fend F, Tzankov A (2021) The pulmonary pathology of COVID-19. Virchows Arch 478(1):137–150

81. Borczuk AC, Salvatore SP, Seshan SV, Patel SS, Bussel JB, Mostyka M et al (2020) COVID-19 pulmonary pathology: a multi-institutional autopsy cohort from Italy and New York City. Mod Pathol 33(11):2156–2168

82. Datta PK, Liu F, Fischer T, Rappaport J, Qin X (2020) SARS-CoV-2 pandemic and research gaps: understanding SARS-CoV-2 interaction with the ACE2 receptor and implications for therapy. Theranostics 10(16):7448–7464

83. Mikhaleva L, Chernayev A, Samsonova M, Zayratyants O, Kakturskiy L, Vasyukova O et al (2021) Pathological features in 100 deceased patients with COVID-19 in correlation with clinical and laboratory data. Pathol Oncol Res. https://doi.org/10.3389/pore.2021.1609900

84. Polak SB, Van Gool IC, Cohen D, von der Thüsen JH, van Paassen J (2020) A systematic review of pathological findings in COVID-19: a pathophysiological timeline and possible mechanisms of disease progression. Mod Pathol 33(11):2128–2138

85. Halperin JA, Taratuska A, Nicholson-Weller A (1993) Terminal complement complex C5b–9 stimulates mitogenesis in 3T3 cells. J Clin Investig 91(5):1974–1978

86. Li S, Zhang H, Li W, Zhai J, Li X, Zheng C (2024) The role of SARS-CoV-2 ORF7a in autophagy flux disruption: implications for viral infection and pathogenesis. Autophagy 20(6):1449–1451

87. Li S, Li X, Liang H, Yu K, Zhai J, Xue M et al (2023) SARS-CoV-2 ORF7a blocked autophagy flux by intervening in the fusion between autophagosome and lysosome to promote viral infection and pathogenesis. J Med Virol 95(11):e29200

88. Zhan Y, Ye L, Ouyang Q, Yin J, Cui J, Liu K et al (2023) The binding profile of SARS-CoV-2 with human leukocyte antigen polymorphisms reveals critical alleles involved in immune evasion. J Med Virol 95(9):e29113

89. Kumar J, Dhyani S, Kumar P, Sharma NR, Ganguly S (2023) SARS-CoV-2–encoded ORF8 protein possesses complement inhibitory properties. J Biol Chem 299(3):102930

90. Ville S, Le Bot S, Chapelet-Debout A, Blancho G, Fremeaux-Bacchi V, Deltombe C et al (2021) Atypical HUS relapse triggered by COVID-19. Kidney Int 99(1):267–268

91. Kaufeld J, Reinhardt M, Schröder C, Bräsen JH, Wiech T, Brylka P et al (2021) Atypical hemolytic and uremic syndrome triggered by infection with SARS-CoV2. Kidney Int Rep 6(10):2709–2712

92. Otieno SB, Altahan A, Kaweeta F, Karri S, Alnoor F, Johnson R (2021) Severe hemolysis in a COVID-19 patient with paroxysmal nocturnal hemoglobinuria. Case Rep Hematol 2021:6619182

93. Hines A, Hakim N, Barrientos J (2021) COVID-19 infection presenting as paroxysmal nocturnal hemoglobinuria. Clin Case Rep 9(8):e04636

94. Uwatoko R, Shindo M, Hashimoto N, Iio R, Ueda Y, Tatematsu Y et al (2023) Relapse of atypical hemolytic uremic syndrome triggered by COVID-19: a lesson for the clinical nephrologist. J Nephrol. https://doi.org/10.1007/s40620-023-01595-y